

Magnetic-field tuned anisotropy in superconducting $\text{Rb}_x\text{Fe}_{2-y}\text{Se}_2$

S. Bosma,^{1,*} R. Puzniak,² A. Krzton-Maziopa,³ M. Bendele,^{1,4}
E. Pomjakushina,³ K. Conder,³ H. Keller,¹ and S. Weyeneth^{1,†}

¹*Physik-Institut der Universität Zürich, Winterthurerstrasse 190, CH-8057 Zürich, Switzerland*

²*Institute of Physics, Polish Academy of Sciences,*

Aleja Lotników 32/46, PL-02-668 Warsaw, Poland

³*Laboratory for Developments and Methods, Paul Scherrer Institute, CH-5232 Villigen PSI, Switzerland*

⁴*Laboratory for Muon Spin Spectroscopy, Paul Scherrer Institute, CH-5232 Villigen PSI, Switzerland*

The anisotropic superconducting properties of a $\text{Rb}_x\text{Fe}_{2-y}\text{Se}_2$ single crystal with $T_c \simeq 32$ K were investigated by means of SQUID and torque magnetometry, probing the effective magnetic penetration depth λ_{eff} and the penetration depth anisotropy γ_λ . Interestingly, γ_λ is found to be temperature independent in the superconducting state, but strongly field dependent: $\gamma_\lambda(0.2 \text{ T}) < 4$ and $\gamma_\lambda(1.4 \text{ T}) > 8$. This unusual anisotropic behavior, together with a large zero-temperature $\lambda_{\text{eff}}(0) \simeq 1.8 \mu\text{m}$, is possibly related to a superconducting state heavily biased by the coexisting antiferromagnetic phase.

PACS numbers: 74.70.Xa, 74.25.Ha, 74.25.Bt, 74.25.Op

I. INTRODUCTION

With the discovery of superconductivity in $\text{LaFeAsO}_{1-x}\text{F}_y$,¹ a new family of iron-based high-temperature superconductors was found. Its simplest member is FeSe_{1-x} , which consists of a stack of FeSe layers.² Its superconducting transition temperature $T_c \simeq 8$ K increases drastically with external pressure, reaching $T_c(8 \text{ GPa}) \simeq 36$ K.^{2,3} Interestingly, a similar high $T_c \simeq 30$ K is attained in the iron-selenide family $A_x\text{Fe}_{2-y}\text{Se}_2$ by intercalating alkali atoms ($A = \text{K}, \text{Rb}, \text{Cs}$) between the FeSe layers.^{4–6} However, T_c is found to decrease with pressure and is fully suppressed at 9 GPa for $\text{K}_x\text{Fe}_{2-y}\text{Se}_2$ (Ref. 7) and at 8 GPa for $\text{Cs}_x\text{Fe}_{2-y}\text{Se}_2$.⁸ The critical temperature is almost insensitive to pressure below 1 GPa, suggesting that T_c is almost independent of small variations of the lattice constants. This provides an opportunity to study the temperature dependence of physical quantities without being affected by changes of the lattice constants due to thermal expansion. Early μSR experiments on $\text{Cs}_x\text{Fe}_{2-y}\text{Se}_2$ indicate that superconductivity and antiferromagnetism coexist on microscopic length scales.⁹ The Néel temperature $T_N \approx 500$ K (Ref. 10) of $\text{K}_{0.8}\text{Fe}_{2-y}\text{Se}_2$ is substantially higher than $T_c \simeq 30$ K. Several experiments point towards nanoscale phase separation between superconducting, vacancy-disordered domains and vacancy ordered antiferromagnetic (AFM) domains.^{11–14} In contrast to the slightly hole doped FeSe_{1-x} , the intercalation of alkali ions A into the FeSe structure introduces a large amount of electrons into the system.¹⁵ Other experiments¹⁶ suggested that this highly electron doped system contains no hole-like sheets at the Fermi surface, and thus electron scattering between hole and electron-like bands is impossible.¹⁵ Moreover, Fe vacancies in the crystalline structure order at $\simeq 600$ K.¹⁷ In $\text{K}_x\text{Fe}_{2-y}\text{Se}_2$, the presence of vacancies appears detrimental to superconductivity.¹⁸

This intriguing microscopic coexistence of vacancy ordering, antiferromagnetism, and superconductivity in $A_x\text{Fe}_{2-y}\text{Se}_2$ points to an unconventional thermodynamic behavior of the superconducting state.

Recently, the lower critical field H_{c1} was investigated in tetragonal $\text{K}_x\text{Fe}_{2-y}\text{Se}_2$ for magnetic fields H along different crystallographic directions, *i.e.* parallel to the ab -plane and parallel to the c -axis,^{19,20} revealing a surprisingly low and isotropic $\mu_0 H_{c1} \simeq 0.3$ mT. Invoking the phenomenological relation between H_{c1} and the effective magnetic penetration depth λ_{eff} for an isotropic superconductor $\mu_0 H_{c1} = \Phi_0(\ln \kappa + 0.5)/(4\pi\lambda_{\text{eff}}^2)$,²¹ a value of $\lambda_{\text{eff}}(0) \simeq 1.6 - 1.8 \mu\text{m}$ is obtained (assuming an approximate Ginzburg-Landau parameter $\kappa \sim 100 - 200$). This low field estimate of λ_{eff} deviates remarkably from the small in-plane magnetic penetration depth $\lambda_{ab}(0) \simeq 0.29 \mu\text{m}$ derived from NMR experiments at 8.3 T on a similar sample.²² Moreover, the numerous observations of an anisotropic vortex lattice in high magnetic fields^{19,22–24} contrast with the isotropic behavior of H_{c1} in low magnetic fields. In order to illuminate this intriguing field dependence of the superconducting properties, we performed a detailed magnetic study of $\text{Rb}_x\text{Fe}_{2-y}\text{Se}_2$.

II. CRYSTAL GROWTH

A $\text{Rb}_x\text{Fe}_{2-y}\text{Se}_2$ single crystal with composition $\text{Rb}_{0.77(2)}\text{Fe}_{1.61(3)}\text{Se}_2$ as refined by X-ray fluorescence was grown from a melt by the Bridgman method, using a presynthesised ceramic precursor of $\text{FeSe}_{0.98}$ and metallic rubidium. For the precursor synthesis high purity (at least 99.99% Alfa) powders of iron and selenium were mixed in the molar proportion 1 Fe : 0.98 Se and pressed into a rod. This nominal stoichiometry, chosen on the basis of our previous studies²⁵ of the Fe-Se chemical phase diagram, provides an iron selenide of pure tetragonal phase. The mixture was prereacted in a sealed silica am-

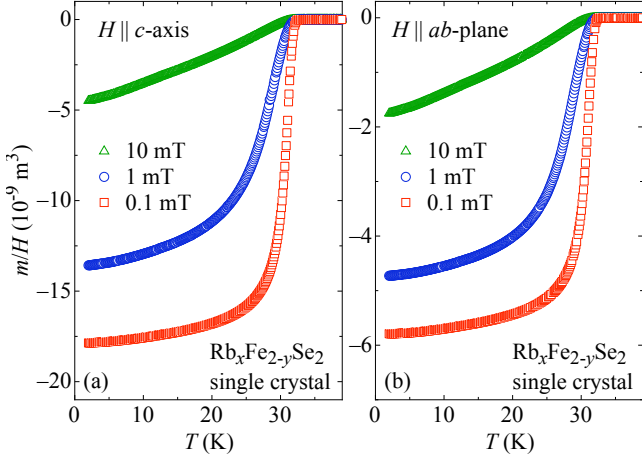


FIG. 1. (Color online) Zero-field cooled measurements of m/H of single crystal $\text{Rb}_x\text{Fe}_{2-y}\text{Se}_2$ for (a) $H \parallel c$ -axis and (b) $H \parallel ab$ -plane. The change of vortex penetration with temperature is very similar for both directions, consistent with an isotropic $\mu_0 H_{c1} \lesssim 0.3$ mT. The sharp transition at $T_c \simeq 32$ K demonstrates the high quality of the crystal. Due to demagnetization the magnitude of m/H varies by a factor of ~ 3 for both orientations. A rough estimation of the demagnetization factors from the sample dimensions yields $0.05 < N^{\parallel ab} < 0.3$ and $N^{\parallel c} \sim 0.65$.

poule at 700 °C for 15 hours and then grounded in an inert atmosphere, pressed again into a rod, sealed in an evacuated double wall quartz ampoule and resintered at 700 °C. After 48 hours the furnace was cooled down to 400 °C and kept at this temperature for 36 hours more. For the single crystal growth a piece of the Fe-Se rod was sealed in an evacuated silica Bridgman ampoule with an appropriate amount of pure alkali metal placed in an additional thin silica tube; 5% excess of Rb was added to compensate its loss during synthesis. The Bridgman ampoule was sealed in another protecting evacuated quartz tube. The ampoule was heated at 1030 °C for 2 hours for homogenization, followed by cooling down the melt to 750 °C at a rate of 6 °C/h. Finally, the furnace was cooled down to room temperature at a rate of 200 °C/h. After synthesis the ampoules were transferred to a He-glove box and opened there to protect the crystal from oxidation in the air.

III. MAGNETIC MEASUREMENTS

The superconducting properties of the plate-like crystal of dimensions $\sim 5 \times 1 \times 0.2$ mm³ (thickness of 0.2 mm along the c -axis) were characterized with a *Quantum Design* MPMS XL SQUID magnetometer. The temperature dependence of m/H , where m is the magnetic moment is shown in Fig. 1 for various magnetic fields H applied after zero-field cooling. The onset transition temperature for this sample is estimated to be $T_c \simeq 32$ K. For both studied orientations (parallel to the c -axis shown in

Fig. 1a, and parallel to the ab -plane shown in Fig. 1b), the magnetic properties are very similar. For $\mu_0 H = 0.1$ mT a sharp diamagnetic transition is observed for both field orientations. In higher fields, the diamagnetism is rapidly suppressed, indicating that $\mu_0 H_{c1}$ for $\text{Rb}_x\text{Fe}_{2-y}\text{Se}_2$ is very low ($\mu_0 H_{c1} \lesssim 0.3$ mT, including demagnetizing field correction.²⁶)

A small piece of of rectangular shape and approximate dimensions $150 \times 150 \times 90$ μm^3 was cleaved off the above $\text{Rb}_x\text{Fe}_{2-y}\text{Se}_2$ single crystal. Magnetic torque investigations were carried out using a home-made magnetic torque sensor.²⁷ For a uniaxial superconductor like tetragonal $\text{Rb}_x\text{Fe}_{2-y}\text{Se}_2$, the angular dependence of the

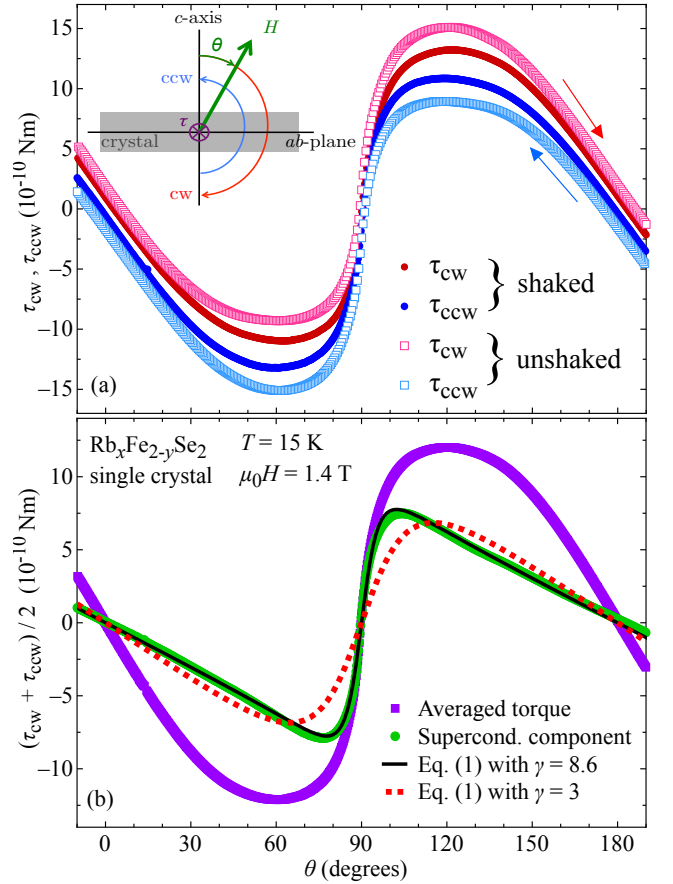


FIG. 2. (Color online) Angular dependent torque of single-crystal $\text{Rb}_x\text{Fe}_{2-y}\text{Se}_2$ measured at 15 K and 1.4 T. (a) Comparison of unshaked and shaken magnetic torque. The unshaked red data τ_{cw} (blue data τ_{ccw}) are gathered by turning H clockwise (counter-clockwise) around the sample. The inset explains schematically the field configuration during the experiment. The shaken data are obtained by applying a transverse AC field, yielding reduced irreversibility and enhanced data quality. (b) Angular dependence of the shaken magnetic torque averaged for both directions. The green curve is the superconducting component of the signal, obtained after subtracting the background as explained in the text. A fit by Eq. (1) yields $\gamma_\lambda(15 \text{ K}, 1.4 \text{ T}) \simeq 8.6$ (black line). For comparison, the red dotted line is calculated with a fixed $\gamma_\lambda = 3$.

magnetic torque $\vec{\tau} = \vec{m} \times \mu_0 \vec{H}$ in the London approximation ($H_{c1} < H < H_{c2}$) can be written according to²⁸

$$\tau(\theta) = -\frac{V\Phi_0 H \gamma_\lambda^{2/3}}{16\pi\lambda_{\text{eff}}^2} \left(1 - \frac{1}{\gamma_\lambda^2}\right) \cdot \frac{\sin(2\theta)}{\epsilon(\theta)} \ln \left(\frac{\eta H_{c2}^{\parallel c}}{\epsilon(\theta)H} \right). \quad (1)$$

Here θ is the angle between H and the crystallographic c -axis, $\epsilon(\theta) = [\cos^2(\theta) + \gamma_\lambda^{-2} \sin^2(\theta)]^{1/2}$ is the angular scaling function, $H_{c2}^{\parallel c}$ is the c -axis upper critical field, and η is a dimensionless parameter of the order of unity. Without loss of generality η is restricted to 1 within this work.²⁹ The anisotropy parameter $\gamma_\lambda = \lambda_c/\lambda_{ab}$ is the ratio of the out-of-plane and in-plane magnetic penetration depths, whereas $\lambda_{\text{eff}} = (\lambda_{ab}^2 \lambda_c)^{1/3}$ denotes the effective magnetic penetration depth. It is possible that our sample presents phase separation between superconducting non-magnetic regions and antiferromagnetic, non-superconducting regions, with a domain size smaller than the penetration depth.¹¹ In that case, applying the Kogan model yields a λ_{eff} which may be renormalized to a larger value than the superconducting parameter $(\lambda_{ab}^2 \lambda_c)^{1/3}$. The field penetrates more easily in this phase separated material, and the Kogan model yields an “averaged” effective bulk penetration depth. The good agreement between Eq. (1) and the data (Fig. 2b) shows that the Kogan model is still useful, albeit with a broader interpretation of its parameters.

The magnetic torque experiments at various T and H were performed by turning H around the sample in a plane containing the c -axis (see inset of Fig. 2a), and measuring the resulting torque. As an example, Fig. 2a shows the angular dependence of the torque signal measured at 15 K in 1.4 T. Note that the torque signal is affected by an angular irreversibility between the clockwise (τ_{cw}) and counter-clockwise (τ_{ccw}) branches. Such irreversible angular dependent torque signals are usually observed in hard superconductors due to vortex pinning.^{30,31} Due to the tetragonal structure of $\text{Rb}_x\text{Fe}_{2-y}\text{Se}_2$, twinning in the crystal manifests itself in the results only through pinning on the twin boundaries, and all in-plane parameters are not separated along a - and b - axes in the analysis. In this work, the so-called vortex-shaking technique³² was successfully applied to reduce irreversibility, allowing a more reliable determination of the superconducting parameters. This was done by applying a small AC field orthogonal to H in order to enhance the vortex relaxation towards thermodynamic equilibrium. As seen in Fig. 2a the vortex shaking clearly reduces the irreversible component, especially for H close to the ab -plane. In Fig. 2b the average torque $\tau = (\tau_{\text{cw}} + \tau_{\text{ccw}})/2$ is presented. The torque signal consists of a superconducting component described by Eq. (1) and a magnetic background component $\tau_{\text{BG}} = -(\chi_{ab} - \chi_c)V\mu_0 H^2 \sin(2\theta)/2$. The variables χ_c and χ_{ab} denote the magnetic susceptibilities along the crystallographic axes. Here $\chi_{ab} > \chi_c$ (as also mentioned in Ref. 22) and τ_{BG} is large, consistent with a bulk antiferromagnetic phase having the magnetic moments aligned along the c -axis.^{9,17} The subtraction

of this antiferromagnetic background can be either performed by adding a sinusoidal component in the fitting routine of Eq. (1), or by directly removing the symmetric sinusoidal component of the data as discussed in Ref. 31. All results presented in this work are independent of the background treatment.

The parameters $H_{c2}^{\parallel c}$, γ_λ , and λ_{eff} can be extracted simultaneously by analyzing the magnetic torque data with Eq. (1). However, in order to reduce the amount of free fit parameters, $H_{c2}^{\parallel c}$ was fixed according to a Werthamer-Helfand-Hohenberg (WHH) temperature dependence.³³ The slope $dH_{c2}^{\parallel c}/dT$ at T_c was fixed to ~ -1 T/K, in concordance with resistivity results of a similar sample.²⁴ Small variations in $dH_{c2}^{\parallel c}/dT$ do not affect the results of the analysis, since H_{c2} contributes only logarithmically in Eq. (1) and has no weight in the determination of γ_λ and λ_{eff} in low magnetic fields.³¹ Magnetic torque curves with the antiferromagnetic background subtracted are presented in Fig. 3 for various T (Fig. 3a) and H (Fig. 3b). The insets show the normalized magnetic torque $\tau_{\text{norm}} = \tau(\theta)/\max[\tau(\theta)]$ close to the ab -plane. A change of the shape of $\tau_{\text{norm}}(\theta)$ qualitatively reflects a change of γ_λ . Note that the slope of τ_{norm} vs. θ changes strongly with H , but not with T . This demonstrates that γ_λ is field dependent, but not temperature dependent. As the field direction is approaching the ab -plane, the screening currents start to flow not only in plane, but also out of plane, which makes the torque depend strongly on λ_{ab} and λ_c in this angular region. The temperature and field effect on the anisotropy γ_λ are consequently already visible on the data taken around the ab -plane, independently of the strict validity of Eq. (1) in a phase separated material.

The temperature dependence of λ_{eff} presented in Fig. 4a can be fitted with the empirical power law $\lambda_{\text{eff}}^{-2}(T) = \lambda_{\text{eff}}^{-2}(0)[1 - (T/T_c)^n]$ with $T_c \simeq 32$ K, $n \simeq 5.2$ and $\lambda_{\text{eff}}(0) \simeq 1.8$ μm . This rather large value of the effective penetration depth may be due to phase separation, as mentioned above. The value of n is quite large compared to what is expected from the two-fluid model the fitting expression comes from. This might be related to phase separation, as the links between superconducting domains could depend on temperature, changing the temperature dependence of the penetration depth. Figure 4b shows $\gamma_\lambda(T)$ for various H . It is almost temperature independent between T_c and $T_c/2$ for all fields studied. The slight drop observed at higher temperatures in 1.4 T may be due to the proximity of the transition, which decreases the superconducting signal. The increase of γ at 1.4 T at low temperatures is most likely due to pinning effects.³⁴ Most importantly, a remarkable monotonous field dependence of γ_λ is observed (Fig. 4d), with the strongest dependence in the lowest fields. In low fields, $\gamma_\lambda(0.2 \text{ T}) \simeq 3.5$. An extrapolation of the measured values of γ_λ towards zero field yields $\gamma_\lambda(0 \text{ T}) \sim 1 - 2$. In Fig. 4c the field dependence of $\lambda_{\text{eff}}(H)$ is shown for various T . The effective penetration depth $\lambda_{\text{eff}}(H)$ tends to

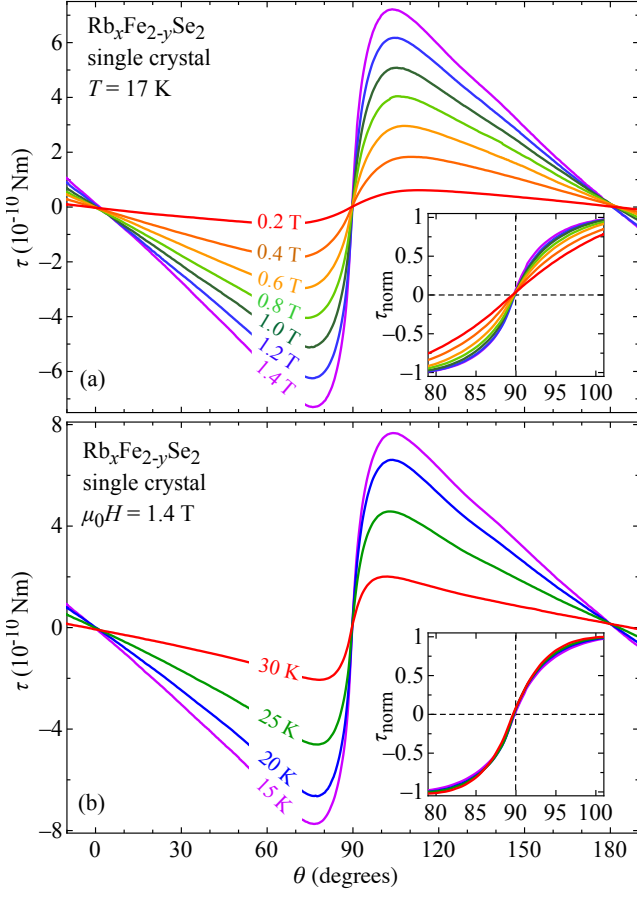


FIG. 3. (Color online) Angular dependence of the superconducting component of the magnetic torque of $\text{Rb}_x\text{Fe}_{2-y}\text{Se}_2$. (a) Magnetic torque at 17 K for various magnetic fields. (b) Magnetic torque at 1.4 T for various temperatures. The insets in both panels show the evolution of τ_{norm} close to the ab -plane.

a constant value for $\mu_0 H \geq 1$ T for all studied T .

IV. DISCUSSION

The extrapolated $\lambda_{\text{eff}}(0) \simeq 1.8 \mu\text{m}$ is surprisingly large compared to that of other iron-based superconductors. In the related iron selenide $\text{FeSe}_{0.5}\text{Te}_{0.5}$ a much lower value of $\lambda_{\text{eff}}(0) \simeq 0.7 \mu\text{m}$ was reported.³⁵ However, for $\text{Rb}_x\text{Fe}_{2-y}\text{Se}_2$ such a large $\lambda_{\text{eff}}(0)$ is consistent with the very small $\mu_0 H_{c1} \lesssim 0.3$ mT observed in this work and in $\text{K}_x\text{Fe}_{2-y}\text{Se}_2$ by others.¹⁹ The small $\gamma_\lambda(0 \text{ T}) \sim 1 - 2$ at very low fields is also in agreement with an isotropic H_{c1} . The increase of $\gamma_\lambda = \lambda_c/\lambda_{ab}$ with H and the field independent $\lambda_{\text{eff}} = (\lambda_{ab}^2 \lambda_c)^{1/3}$ imply that $\lambda_{ab} = \lambda_{\text{eff}} \gamma_\lambda^{-1/3}$ decreases with increasing H . This is consistent with the high-field NMR result.²² The small high-field value of λ_{ab} reported in Ref. 22, in combination with the saturating $\lambda_{\text{eff}}(H)$ and the field dependence of $\gamma_\lambda(H)$ observed here, suggests that

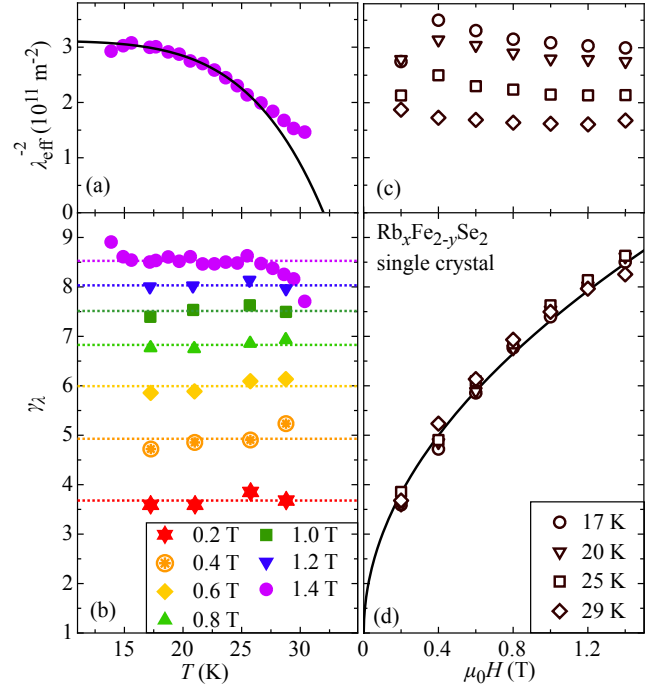


FIG. 4. (Color online) Summary of all the results obtained by analyzing the experimental torque signal of $\text{Rb}_x\text{Fe}_{2-y}\text{Se}_2$ with Eq. (1). (a) Temperature dependence of $\lambda_{\text{eff}}^{-2}$. The line is a power law fit to the data at 1.4 T. (b) Temperature dependence of γ_λ for various fields, showing that γ_λ is strongly increasing with H , but is almost independent of T . The dotted lines represent the average γ_λ for each field. (c) Field dependence of $\lambda_{\text{eff}}^{-2}$ for various temperatures. (d) Field dependence of γ_λ for various T . The black line is a guide to the eye.

γ_λ continues to increase at higher fields. Note that the anisotropy of ~ 3 (Ref. 23) observed in very high fields by upper critical field measurements cannot be directly compared with the magnetic penetration depth anisotropy γ_λ investigated here, because in general $H_{c2}^{\parallel ab}/H_{c2}^{\parallel c} = \xi_{ab}/\xi_c = \gamma_\xi \neq \gamma_\lambda$.³¹

A field dependent γ_λ might be associated with a complex band structure, since in the case of multiple superconducting gaps originating from different bands the superconducting screening currents, related to λ_{ab} and λ_c , may give rise to an unusual behavior of γ_λ . A similar behavior was observed in MgB_2 , where the two-gap excitation spectrum yields a strongly field dependent anisotropy.^{36,37} In MgB_2 , as the field increases, the gap from the 3D σ -band is closed, so the main part of the superconducting fluid density comes from the 2D π -band. The 2D character of the remaining band implies a larger anisotropy.

Band structure calculations³⁸⁻⁴⁰ in $\text{A}_x\text{Fe}_{2-y}\text{Se}_2$ yield multiple bands, with four 2D sheets on the sides of the Brillouin zone and one cylindrical sheet at the center. Depending on doping, this cylinder can be split into two 3D cones in $\text{K}_{0.8}\text{Fe}_2\text{Se}_2$,³⁸ which are completely

detached (3D) in the calculation of Ref. 39, although when the authors use experimental lattice parameters these cones are replaced by a cylinder (2D). According to Ref. 40, the center band is a cylinder. In CsFe_2Se_2 and $\text{Cs}_{0.8}\text{Fe}_2\text{Se}_2$, this band consists in two almost detached cones.³⁸ In $\text{Tl}_{0.58}\text{Rb}_{0.42}\text{Fe}_{1.72}\text{Se}_2$,⁴¹ two gaps of different amplitudes were observed on the side and center bands, but the candidate for a 3D inner band was too small for a gap to be observed. It is therefore not yet clear whether for $\text{Rb}_x\text{Fe}_{2-y}\text{Se}_2$ with the doping used in this work a 3D band is present. Clearly, more material specific work is needed in order to clarify the interplay between multiband superconductivity and the anisotropy of $\text{Rb}_x\text{Fe}_{2-y}\text{Se}_2$. However, if a 2D-3D band scenario is the origin of the field dependence of the anisotropy of $\text{Rb}_x\text{Fe}_{2-y}\text{Se}_2$, it must be temperature dependent as well,³⁶ which is not the case according to Fig. 4d.

The temperature independent γ_λ suggests that the origin of its field dependence is not related to the superconducting gap energy, which is strongly temperature dependent in the examined temperature range. However, there is one energy scale which is almost temperature independent in the superconducting state: the Néel temperature $T_N \approx 500$ K.¹⁰ A superconductor coexisting with an antiferromagnetic phase is expected to behave in a peculiar way, although the temperature range studied here is far too low to excite any change in this strongly coupled antiferromagnet. However, magnetic field modifications can lead to changes in the domain structure, and therefore changes of coupling between superconducting areas. This could result in variations of the “averaged” effective anisotropy. As was shown for various iron-based superconductors, the lattice parameters, in particular the pnictogen height in the iron-pnictides, are directly related to superconductivity.⁴² Importantly, such scaling also works for the iron-selenide layer.^{5,42} It is also possible

that magnetostrictive effects, which are expected to increase with magnetic field, may influence the lattice parameters and by that the anisotropy of the system. In such a case the strong curvature of $H_{c2}(T)$ in the vicinity of T_c often observed in pnictides/chalcogenides may be explained by the change of T_c with H caused by the change of pnictogen height.

V. SUMMARY

In summary, we present an investigation of the magnetic properties of $\text{Rb}_x\text{Fe}_{2-y}\text{Se}_2$ revealing a strong field dependence of γ_λ ranging from $\gamma_\lambda(0.2 \text{ T}) < 4$ to $\gamma_\lambda(1.4 \text{ T}) > 8$. This behavior stands out among other iron-based superconductors, consistent with the singular coexistence of magnetic ordering and superconductivity. In accordance with lower critical field measurements, our data suggest that in very low fields $\gamma_\lambda(0 \text{ T}) \sim 1 - 2$. At 1.4 T the effective magnetic penetration depth is $\lambda_{\text{eff}}(0) \simeq 1.8 \mu\text{m}$. The vortex phase in $\text{Rb}_x\text{Fe}_{2-y}\text{Se}_2$ is best described by an isotropic three dimensional state in low fields which becomes strongly anisotropic with increasing field. In this respect the novel iron-selenide $\text{Rb}_x\text{Fe}_{2-y}\text{Se}_2$ could be a potential candidate for magnetic-field tuned applications of superconductivity.

VI. ACKNOWLEDGEMENTS

This work was supported by the Swiss National Science Foundation, in part by the NCCR program MaNEP and the Sciex-NMSch (project code 10.048), and by National Science Centre (Poland) based on decision No. DEC-2011/01/B/ST3/02374.

* sbosma@physik.uzh.ch

† wstephen@physik.uzh.ch

¹ Y. Kamihara, T. Watanabe, M. Hirano, and H. Hosono, *J. Am. Chem. Soc.* **130**, 3296 (2008).

² F.-C. Hsu, J.-Y. Luo, K.-W. Yeh, T.-K. Chen, T.-W. Huang, P. M. Wu, Y.-C. Lee, Y.-L. Huang, Y.-Y. Chu, D.-C. Yan, and M.-K. Wu, *P. Natl. A. Sci. USA* **105**, 14262 (2008).

³ S. Margadonna, Y. Takabayashi, Y. Ohishi, Y. Mizuguchi, Y. Takano, T. Kagayama, T. Nakagawa, M. Takata, and K. Prassides, *Phys. Rev. B* **80**, 064506 (2009).

⁴ J. Guo, S. Jin, G. Wang, S. Wang, K. Zhu, T. Zhou, M. He, and X. Chen, *Phys. Rev. B* **82**, 180520 (2010).

⁵ A. Krzton-Maziopa, Z. Shermadini, E. Pomjakushina, V. Pomjakushin, M. Bendele, A. Amato, R. Khasanov, H. Luetkens, and K. Conder, *J. Phys.: Condens. Matter* **23**, 052203 (2011).

⁶ C.-H. Li, B. Shen, F. Han, X. Zhu, and H.-H. Wen, *Phys. Rev. B* **83**, 184521 (2011).

⁷ J. Guo, X. Chen, C. Zhang, J. Guo, X. Chen, Q. Wu, D. Gu, P. Gao, X. Dai, L. Yang, H.-k. Mao, L. Sun, and Z. Zhao, *ArXiv e-prints* (2011), arXiv:1101.0092 [cond-mat.supr-con].

⁸ G. Seyfarth, D. Jaccard, P. Pedrazzini, A. Krzton-Maziopa, E. Pomjakushina, K. Conder, and Z. Shermadini, *Solid State Commun.* **151**, 747 (2011).

⁹ Z. Shermadini, A. Krzton-Maziopa, M. Bendele, R. Khasanov, H. Luetkens, K. Conder, E. Pomjakushina, S. Weyeneth, V. Pomjakushin, O. Bossen, and A. Amato, *Phys. Rev. Lett.* **106**, 117602 (2011).

¹⁰ R. H. Liu, X. G. Luo, M. Zhang, A. F. Wang, J. J. Ying, X. F. Wang, Y. J. Yan, Z. J. Xiang, P. Cheng, G. J. Ye, Z. Y. Li, and X. H. Chen, *EPL (Europhysics Letters)* **94**, 27008 (2011).

¹¹ A. Ricci, N. Poccia, G. Campi, B. Joseph, G. Arrighetti, L. Barba, M. Reynolds, M. Burghammer, H. Takeya, Y. Mizuguchi, Y. Takano, M. Colapietro, N. L. Saini, and A. Bianconi, *Phys. Rev. B* **84**, 060511 (2011).

- ¹² B. Shen, B. Zeng, G. F. Chen, J. B. He, D. M. Wang, H. Yang, and H. H. Wen, *EPL (Europhysics Letters)* **96**, 37010 (2011).
- ¹³ V. Ksenofontov, G. Wortmann, S. Medvedev, V. Tsurkan, J. Deisenhofer, A. Loidl, and C. Felser, *ArXiv e-prints* (2011), arXiv:1108.3006 [cond-mat.supr-con].
- ¹⁴ Z. Wang, Y. J. Song, H. L. Shi, Z. W. Wang, Z. Chen, H. F. Tian, G. F. Chen, J. G. Guo, H. X. Yang, and J. Q. Li, *Phys. Rev. B* **83**, 140505 (2011).
- ¹⁵ A. L. Ivanovskii, *Physica C* **471**, 409 (2011).
- ¹⁶ Y. Zhang, L. X. Yang, M. Xu, Z. R. Ye, F. Chen, C. He, H. C. Xu, J. Jiang, B. P. Xie, J. J. Ying, X. F. Wang, X. H. Chen, J. P. Hu, M. Matsunami, S. Kimura, and D. L. Feng, *Nat. Mater.* **10**, 273 (2011).
- ¹⁷ W. Bao, Q. Huang, G. F. Chen, M. A. Green, D. M. Wang, J. B. He, X. Q. Wang, and Y. Qiu, *Chin. Phys. Lett.* **28**, 086104 (2011).
- ¹⁸ W. Li, H. Ding, P. Deng, K. Chang, C. Song, K. He, L. Wang, X. Ma, J.-P. Hu, X. Chen, and Q.-K. Xue, *Nat. Phys.*, doi:10.1038/nphys2155 (2011).
- ¹⁹ H. Lei and C. Petrovic, *Phys. Rev. B* **83**, 184504 (2011).
- ²⁰ M. I. Tsindlekht, I. Felner, M. Zhang, A. F. Wang, and X. H. Chen, *Phys. Rev. B* **84**, 052503 (2011).
- ²¹ R. A. Klemm and J. R. Clem, *Phys. Rev. B* **21**, 1868 (1980).
- ²² D. A. Torchetti, M. Fu, D. C. Christensen, K. J. Nelson, T. Imai, H. C. Lei, and C. Petrovic, *Phys. Rev. B* **83**, 104508 (2011).
- ²³ E. D. Mun, M. M. Altarawneh, C. H. Mielke, V. S. Zapf, R. Hu, S. L. Bud'ko, and P. C. Canfield, *Phys. Rev. B* **83**, 100514(R) (2011).
- ²⁴ V. Tsurkan, J. Deisenhofer, A. Günther, H. . Krug von Nidda, S. Widmann, and A. Loidl, *ArXiv e-prints* (2011), arXiv:1107.3932 [cond-mat.supr-con].
- ²⁵ E. Pomjakushina, K. Conder, V. Pomjakushin, M. Bendele, and R. Khasanov, *Phys. Rev. B* **80**, 024517 (2009).
- ²⁶ J. A. Osborn, *Phys. Rev.* **67**, 351 (1945).
- ²⁷ S. Kohout, J. Roos, and H. Keller, *Rev. Sci. Instrum.* **78**, 013903 (2007).
- ²⁸ V. G. Kogan, *Phys. Rev. B* **38**, 7049 (1988).
- ²⁹ S. Bosma, S. Weyeneth, R. Puzniak, A. Erb, A. Schilling, and H. Keller, *Phys. Rev. B* **84**, 024514 (2011).
- ³⁰ S. Weyeneth, R. Puzniak, U. Mosele, N. D. Zhigadlo, S. Katrych, Z. Bukowski, J. Karpinski, S. Kohout, J. Roos, and H. Keller, *J. Supercond. Nov. Magn* **22**, 325 (2009).
- ³¹ S. Weyeneth, R. Puzniak, N. Zhigadlo, S. Katrych, Z. Bukowski, J. Karpinski, and H. Keller, *J. Supercond. Nov. Magn.* **22**, 347 (2009).
- ³² M. Willemin, C. Rossel, J. Hofer, H. Keller, A. Erb, and E. Walker, *Phys. Rev. B* **58**, R5940 (1998).
- ³³ N. R. Werthamer, E. Helfand, and P. C. Hohenberg, *Phys. Rev.* **147**, 295 (1966).
- ³⁴ M. Willemin, A. Schilling, H. Keller, C. Rossel, J. Hofer, U. Welp, W. K. Kwok, R. J. Olsson, and G. W. Crabtree, *Phys. Rev. Lett.* **81**, 4236 (1998).
- ³⁵ M. Bendele, S. Weyeneth, R. Puzniak, A. Maisuradze, E. Pomjakushina, K. Conder, V. Pomjakushin, H. Luetkens, S. Katrych, A. Wisniewski, R. Khasanov, and H. Keller, *Phys. Rev. B* **81**, 224520 (2010).
- ³⁶ M. Angst, R. Puzniak, A. Wisniewski, J. Jun, S. M. Kazakov, J. Karpinski, J. Roos, and H. Keller, *Phys. Rev. Lett.* **88**, 167004 (2002).
- ³⁷ M. Angst and R. Puzniak, "Focus on superconductivity research," (Nova Science Publishers, New York, 2004) Chap. 1, pp. 1–49, arXiv: cond-mat/0305048.
- ³⁸ I. Nekrasov and M. Sadovskii, *JETP Letters* **93**, 166 (2011).
- ³⁹ I. R. Shein and A. L. Ivanovskii, *Physics Letters A* **375**, 1028 (2011).
- ⁴⁰ C. Cao and J. Dai, *Chin. Phys. Lett.* **28**, 057402 (2011).
- ⁴¹ D. Mou, S. Liu, X. Jia, J. He, Y. Peng, L. Zhao, L. Yu, G. Liu, S. He, X. Dong, J. Zhang, H. Wang, C. Dong, M. Fang, X. Wang, Q. Peng, Z. Wang, S. Zhang, F. Yang, Z. Xu, C. Chen, and X. J. Zhou, *Phys. Rev. Lett.* **106**, 107001 (2011).
- ⁴² Y. Mizuguchi, Y. Hara, K. Deguchi, S. Tsuda, T. Yamaguchi, K. Takeda, H. Kotegawa, H. Tou, and Y. Takano, *Supercond. Sci. Tech.* **23**, 054013 (2010).